Optical Topography Measurement of Patterned Wafers

Xavier Colonna de Lega and Peter de Groot

Zygo Corporation, Laurel Brook Road, Middlefield CT 06455, USA
xcolonna@zygo.com

Abstract. We model the measurement process in an interference microscope and derive libraries of signal signatures corresponding to various types of materials and thin film structures. These libraries allow calculating the top surface topography of patterned wafer features as well as the thickness of the underlying top transparent layer with nanometer height resolution. We show applications of the technique to the measurement of trenches etched in SiO_2 films, post-CMP STI patterns and line structures. The results of the optical profiler are in good agreement with AFM and ellipsometer measurements of nearby structures.

Keywords: Surface Topography, Patterned Wafer, Interference Microscopy.
PACS: 42.87.-d Optical testing techniques, 07.60.Ly Interferometers

INTRODUCTION

Low-coherence interference microscopy is the basis for flexible surface profilers that handle rough, optically smooth and discontinuous surfaces.[1,2] Vertical resolution is sub-nanometer with sub-micron lateral resolution for high magnification objectives. Application of such tools to metrology tasks relevant to the semiconductor industry requires solving a number of problems, including dissimilar material effects, transparent films and unresolved features. In this paper we discuss how modeling of the interferometer allows generating signal libraries that provide "true" topography of complex surface structures characteristic of patterned wafers. Example measurements illustrate the benefit of the technique on a number of patterned structures.

INTERFERENCE MICROSCOPY

FIGURE 1 shows a typical low-coherence interference microscope. An extended broadband light source is imaged at the pupil of a microscope objective equipped with a Mirau interferometer. The reference mirror position is adjusted so that high-contrast optical interference fringes are observed at the camera when the sample surface is at best-focus. Owing to the wide spectral range and spatial extent of the source the contrast of these fringes falls off rapidly for object points that are located above or below this plane. The actual measurement is performed by moving the objective and interferometer vertically while recording the intensity pattern at each pixel of the camera. An example signal is shown in FIGURE 2.

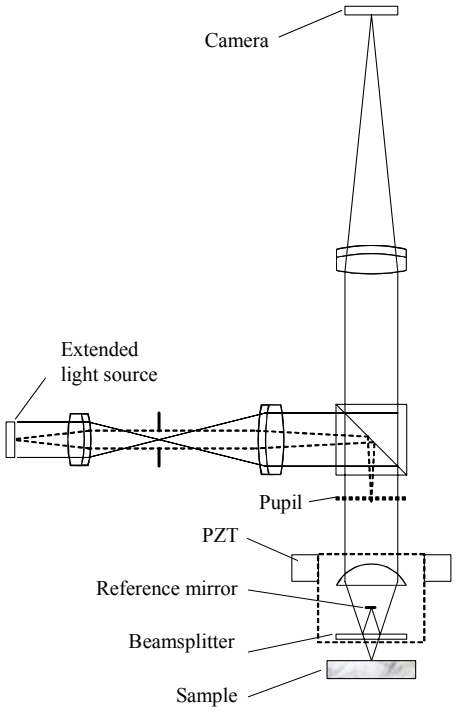

FIGURE 1. Interference microscope.

CP 788, *Characterization and Metrology for ULSI Technology 2005,*
edited by D. G. Seiler, A. C. Diebold, R. McDonald, C. R. Ayre, R. P. Khosla, S. Zollner, and E. M. Secula

The processing of these interference signals relies on both the localization of the interference contrast and phase of the underlying carrier to generate a height map of the profiled object surface. This processing can be advantageously accomplished in the frequency domain to achieve sub-nm resolution.[3]

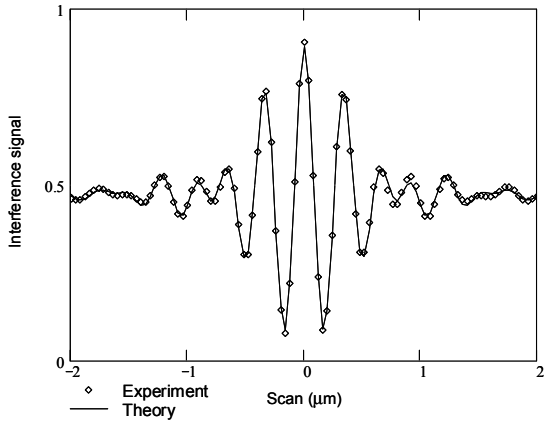

FIGURE 2. Interference signal recorded at a camera pixel for a chromium-coated mirror surface. Experimental data points are shown along with the model-predicted signal.

Application of the technique to transparent thin films becomes trickier when the interference signals created by the various interfaces overlap. This regime corresponds to film thickness smaller than about 1 micrometer. FIGURE 3 shows the interference signal for a 1-μm thick silicon dioxide film grown on a silicon substrate.

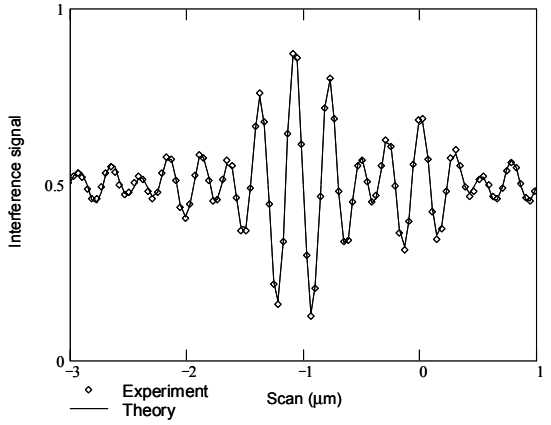

FIGURE 3. Interference signal recorded at a camera pixel for a 1-μm thick SiO_2 film on Si. Experimental data points are shown along with the model-predicted signal.

SIGNAL MODELING FOR COMPLEX STRUCTURES

To properly extract topography information from signals created by multilayer structures we developed a model of the measurement process that includes the properties of the object surface as it is illuminated from a range of directions at various wavelengths.[4,5] The starting point is to consider each source point at the pupil as a source of coherent radiation at a specific wavelength. Because of the detector integration time, different source points are effectively incoherent and the expected signal is the sum of the intensities produced by each source point at each wavelength for each position of the interferometer with respect to the object during a measurement. A source point location at the pupil corresponds to the angle of incidence of the plane wavefront created by this source point at the object. Angle of incidence, wavelength, film thicknesses and material properties are taken into account to calculate the complex reflectivity of the object.[6]

The theoretical model yields the predicted magnitude and phase spectrum of the measured signal in the frequency domain. A benefit of working in this domain is that object height with respect to the interferometer is decoupled from the signal spectral signature that corresponds to a specific structure. Indeed, object height is encoded as a linear phase variation whereas the signature of the object surface is encoded in higher order phase[7,8] and magnitude variations. Another benefit is the computational efficiency of the algorithm, which allows generating libraries of expected signals for various materials and film thicknesses in a reasonable amount of time.

As an example, FIGURE 2 and FIGURE 3 show the match between experimental data and model data for a 100X 0.8NA Mirau interference microscope objective illuminated with a 500-nm LED (27-nm FWHM). The corresponding spectral signatures are shown in FIGURE 4.

SIGNAL LIBRARY-BASED PROFILING

The excellent agreement between experimental data and model signals validates the modeling approach. The next step is to use signal libraries generated as described above to process signals captured when measuring object structures that have

unknown characteristics.[9] In the case of semiconductor structures the available materials and expected structures are known whereas film thickness and top surface topography are the variables of interest. For such measurements each pixel signature is compared to libraries entries. The best matching library signature provides the thickness value(s) of interest. The library phase signature is then subtracted from the measured phase data. The residual linear phase trend provides directly the height of the top object surface in the coordinate system defined by the interferometer.

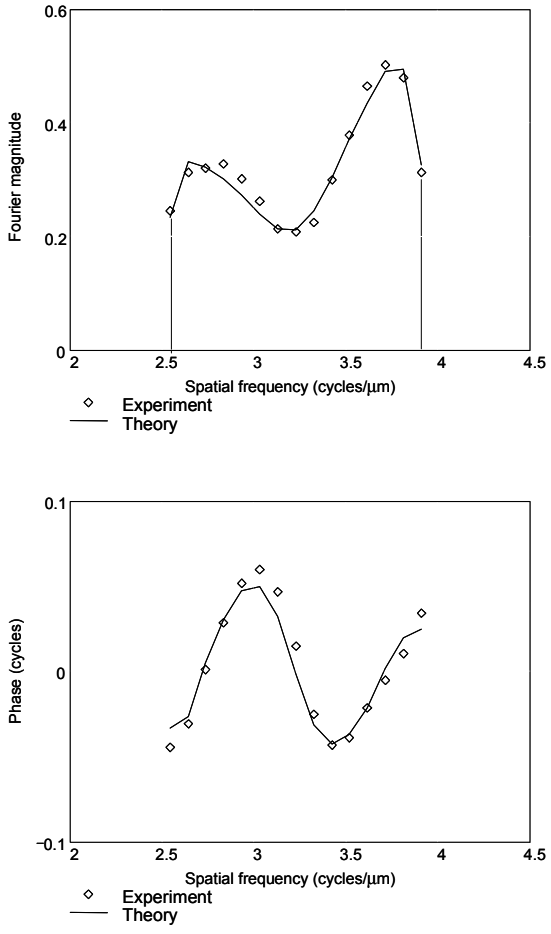

FIGURE 4. Spectral magnitude (top) and phase (bottom) corresponding to the measured and modeled signals shown in FIGURE 3.

APPLICATION EXAMPLES

Film thickness standards

We measured a number of film thickness standards manufactured by VLSI and other companies. The materials are silicon dioxide and silicon nitride on silicon substrates. Signal libraries are created for each type of structure using published refractive index values.[10,11] The results are shown in FIGURE 5. The deviation from the expected slope of 1 is consistent with the difference in refractive indices used to generate the signal libraries and the indices provided by the calibration certificates.[12]

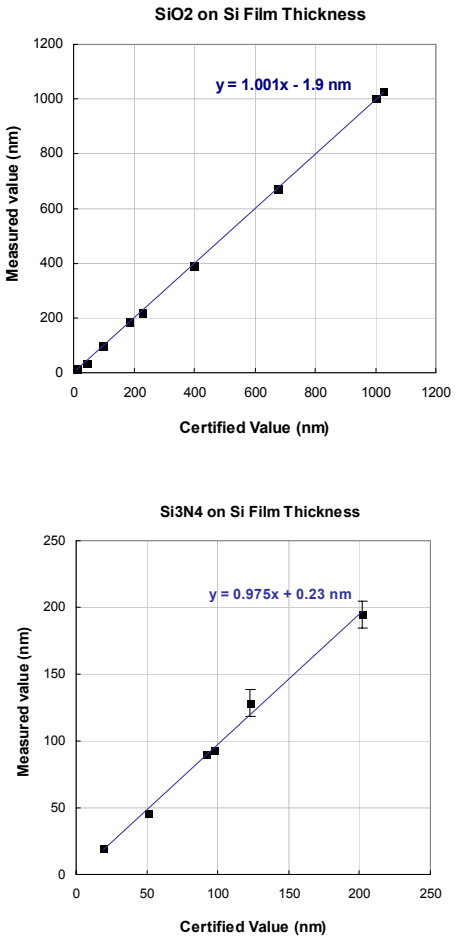

FIGURE 5. Measured film thickness of various film thickness standards. The film materials are SiO_2 (top) and Si_3N_4 (bottom).

Silicon dioxide trenches

The following samples are thermally grown silicon dioxide films on silicon, about 1-µm thick. An etch process was used to create trenches of various widths and depths in the dioxide layer. The profiles shown in FIGURE 6 are derived from measurements of nominally 100-nm deep trenches with a 100X 0.8NA interference objective equipped with a broadband source (100-nm FWHM). The signal library contains samples for silicon dioxide films on silicon with a film thickness ranging from 0 to 1100 nm. The film thickness outside of the trenches is found to be 950 nm. Ellipsometric characterization of these films confirms this value to within one nanometer. Metrology AFM measurements also provide an estimated trench depth value of 96 nm which matches the 95 nm value measured by the optical profiler. Hence, the optical tool measures simultaneously film thickness and surface topography for these samples. The acquisition time is a few seconds for a sampled field of view of 70 x 100 µm.

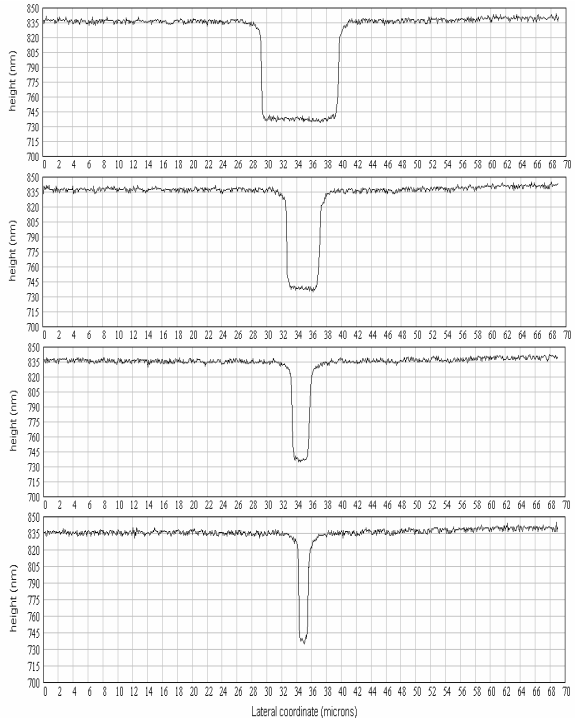

FIGURE 6. Profile of the top surface of an etched SiO_2 film. The film is 950-nm thick. The trench depth is 95 nm. Each profile is 70-µm wide. Horizontal divisions are 2-µm, vertical divisions are 15-nm. Trench width is 10 µm (top profile), 4 µm, 2 µm and 1.5 µm.

STI line patterns

This next example is a 300-mm wafer after CMP during the STI manufacturing phase. The group of lines shown in FIGURE 7 has a 4-µm pitch. The figure shows a 3D rendering of the top surface topography and bottom surface topography calculated using a library of silicon dioxide on silicon signal signatures. We find that the silicon substrate is exposed between the three dioxide-filled trenches but that the dioxide barriers still protrude 70 nm above the top silicon surface. This is an example where the CMP process was not able to planarize fully the wafer.

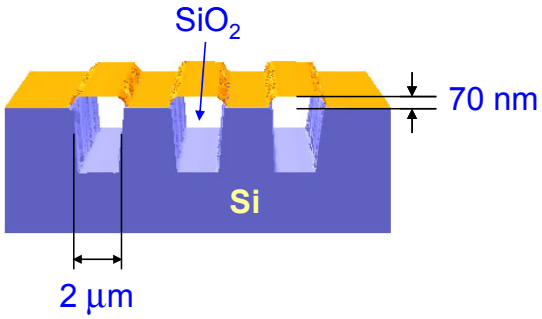

FIGURE 7. 3D rendering of a silicon substrate topography and SiO_2 top surface topography on a post-CMP wafer during the STI manufacturing phase. Trench depth is 480 nm. The SiO_2 barriers protrude 70 nm above the surface of the wafer.

STI structures

For this experiment we measured three post-CMP wafers, again in the STI manufacturing phase. The wafers were nominally, over- and under- polished. Table 1 below shows the height difference between the top of the silicon dioxide and the top of the exposed silicon substrate, measured on large scale structures (10-µm wide). These results are consistent with similar measurements performed with a metrology AFM, except for a 23-nm discrepancy for the over polished wafer (this may have been a different site on the wafer).

TABLE 1. Comparison of AFM and optical profiler data

Wafer type	Optical profiler step height (nm)	AFM step height (nm)
Over polished	- 70	- 47
Nominal CMP	75	70
Under polished	110	111

FIGURE 8 shows a 3D rendering of a measured region on the nominally polished wafer. The field of view is 120 x 90 μm wide. The measured silicon dioxide thickness is about 450 nm.

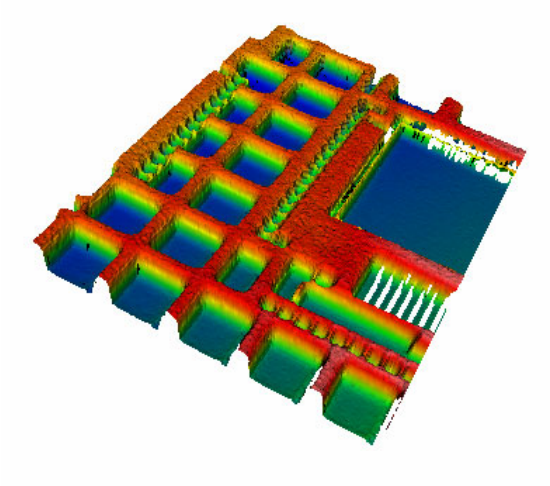

FIGURE 8. 120 x 90 μm area of a patterned wafer post CMP. The lower regions are exposed silicon surrounded by a 450-nm thick layer of SiO_2. The height difference between the two materials is about 75 nm (SiO_2 is higher).

CONCLUSION

Using a general model of interference microscopes we generate interference signature libraries for complex object surface structures. This allows identifying dissimilar materials, measuring their respective thicknesses and providing topography maps of the various interfaces. Agreement with ellipsometric thickness measurements as well as AFM step height measurements confirms the accuracy of the technique on silicon dioxide films. Potential applications include the characterization of wafer surface topography post CMP (STI, damascene Cu, etc). A major benefit of the technique is the simultaneous characterization of surface topography and film thickness at much higher throughput than AFM or ellipsometers.

ACKNOWLEDGMENTS

The authors gratefully acknowledge the contributions of David Grigg, Jim Kramer and Jim Biegen to this work.

REFERENCES

1. M. Davidson, K. Kaufman, I. Mazor, and F. Cohen, "An Application of Interference Microscopy to Integrated Circuit Inspection and Metrology", Proceedings SPIE 775, Integrated circuit metrology, inspection and process control, 233-247 (1987).
2. G. S. Kino and S. S. C. Chim, "Mirau correlation microscope," Appl. Opt. **29**(26), 3775-3783 (1990).
3. P. de Groot, "Method and apparatus for surface topography measurement by spatial-frequency analysis of interferograms," U.S. patent 5,398,113, 14 Mar. 1995.
4. Peter de Groot, Xavier Colonna de Lega, "Signal Modeling for Low-Coherence Height-Scanning Interference Microscopy," Appl. Opt. **43**(25), 4821-4830 (2004).
5. P. de Groot and X. Colonna de Lega, "Signal modeling for modern interference microscopes," Proc. SPIE 5457, 26-34 (2004).
6. M. Born and E. Wolf, Sections 1.5 and 1.6, in *Principles of Optics*, 7th ed., Cambridge: Cambridge University Press, 1999, pp. 38-74.
7. S. W. Kim and G. H. Kim, "Method for measuring a thickness profile and a refractive index using white-light scanning interferometry and recording medium therefore," US Patent 6,545,763B1 (Apr. 8, 2003).
8. S.-W. Kim and G.-H. Kim, "Thickness-profile measurement of transparent thin-film layers by white-light scanning interferometry," Appl. Opt. **38**(28), 5968-5973 (1999).
9. These classes of techniques are covered by published patent applications 20040085544 and 20040189999, assigned to Zygo Corporation.
10. C. M. Herzinger, B. Johs, W. A. McGahan, J. A. Woollam, W. Paulson, "Ellipsometric determination of optical constants for silicon and thermally grown silicon dioxide via a multi-sample, multi-wavelength, multi-angle investigation," J. Appl. Phys. **83**(6), 3323-3336 (1998).
11. H. R. Philipp, "Silicon Nitride (Noncrystalline)," in *Handbook of Optical Constants of Solids*, edited by E. D. Palik, Academic Press, 1985, pp. 771-774.
12. The refractive index values published for Si_3N_4 can vary by as much as 0.02 at visible wavelengths.